# Thermal conductivity of glassy GeTe4 by first-principles molecular dynamics

Assil Bouzid, Hayat Zaoui, Pier Luca Palla, Guido Ori, Mauro Boero, Carlo Massobrio, Fabrizio Cleri, Évelyne Martin

Journal Name

ARTICLE TYPE

Cite this: DOI: 10.1039/xxxxxxxxxx

# Thermal Conductivity of glassy $GeTe_4$ by First-Principles Molecular Dynamics

Assil Bouzid,[a],†, Hayat Zaoui,[b] Pier Luca Palla,[b] Guido Ori,[a] Mauro Boero,[a] Carlo Massobrio,[a] Fabrizio Cleri,[b] and Evelyne Lampin[b]

Received Date
Accepted Date

DOI: 10.1039/xxxxxxxxxx

www.rsc.org/journalname

**A transient thermal regime is achieved in glassy $GeTe_4$ by first-principles molecular dynamics following the recently proposed "approach-to-equilibrium" methodology.[1] The temporal and spatial evolution of the temperature do comply with the time-dependent solution of the heat equation. We demonstrate that the time scales required to create the hot and the cold parts of the system and observe the resulting approach to equilibrium are accessible to first-principles molecular dynamics. Such a strategy provides the thermal conductivity from the characteristic decay time. We rationalize in detail the impact on the thermal conductivity of the initial temperature difference, the equilibration duration, and the main simulation features.**

Molecular dynamics (MD) simulations of thermal properties, e. g. thermal conductivity and interface thermal resistance, give access on equal footing to all the orders of phonon-phonon scattering via the anharmonicity of the interatomic energy landscape, together with relevant atomic-scale details such as surface roughness, point or extended defects, pores or nano-inclusions and interfaces. Using interatomic potentials to describe the interactions, classical molecular dynamics (CMD) has been applied to the calculation of thermal conductivity either via the equilibrium molecular dynamics (EMD) (Green-Kubo[2]) method or the so-called direct method.[3] As a viable and faster alternative, we have developed the approach-to-equilibrium molecular dynamics (AEMD)[1,4] based on the establishment and analysis of thermal transients. This strategy does not require a stationary state to be attained, all information leading to the description of the thermal process being readily available within the molecular dynamics trajectory of the transient. A gain of one order of magnitude in computational time can be estimated for AEMD with respect to stationary approaches.

It appears that the description of the energy landscape and its anharmonic character might not be properly addressed by empirical potentials, resulting in poor predictions of the thermal conductivity. For instance, in crystalline silicon, the thermal conductivity can be largely overestimated.[5–7] The situation can be even worse in the case of interfaces between organic and inorganic materials[8], when the anharmonic regime of the potential energy is sampled by atomic vibrations far from equilibrium, at high pressure/temperature[9], or in the case of complex materials like glasses.[10] To go beyond these limitations and achieve quantitative predictions, a first-principle description of thermal transport via density-functional theory (by using FPMD, first-principles molecular dynamics) is highly desirable. However, FPMD is often characterized by a prohibitive computational cost, limiting typical applications to several hundreds of picoseconds at most for simulations cells hardly containing more than 500 atoms. So far, FPMD has been used in combination with lattice dynamics, under the approximations employed to treat the thermal conductivity of a kinetic gas.[9] The question arises on whether the available stationary approaches are well suited for the study of heat transport within a fully dynamical FPMD scheme. In the

[a] *Université de Strasbourg, CNRS, Institut de Physique et Chimie des Matériaux de Strasbourg, UMR 7504, F-67034 Strasbourg, France.*

† *Present address: Chaire de Simulation à l'Echelle Atomique (CSEA), Ecole Polytechnique Fédérale de Lausanne (EPFL), CH-1015 Lausanne, Switzerland.*

[b] *Univ. Lille, CNRS, Centrale Lille, ISEN, Univ. Valenciennes, UMR 8520 - IEMN, F-59000 Lille, France. E-mail: evelyne.lampin@univ-lille1.fr*

case of the direct method, the supercell dimensions have to be carefully determined either to converge to a bulk thermal conductivity or to allow approaching the convergence via a reliable extrapolation. As for the Green-Kubo method, the definition of energies and currents quantum-mechanically is far from straightforward requiring specific methodological efforts [11]. For these reasons, one would like to turn to AEMD to circumvent these stumbling blocks and obtain a quantitative assessment of thermal transport properties.

On the side of transient methods, early attempts to study a thermal regime by FPMD are due to Luo and Lloyd. [12] These authors have considered crystalline structures of Si, Ge and SiGe containing 64 atoms, showing that a temperature difference between two halves of the system can be obtained by applying a double thermostat. Having in mind AEMD as a viable transient method worth applying, these results are quite instructive since for Si and Ge the distribution of phonon mean free paths (MFPs) extends above the micrometer. [13,14] Therefore, for Si and Ge, no meaningful comparison between experimental thermal conductivities and those stemming from such small supercells can be obtained. Accordingly, to be feasible and rewarding, the applications of AEMD within FPMD have to be not only computationally affordable but also fully compatible with the characteristic spatial lengths inherent in the thermal processes.

In the present letter we achieve this goal for glassy $GeTe_4$ (g-$GeTe_4$), a system widely considered in the context of phase change memory devices. In this material, the heat carriers have very short mean free paths, namely 4-5 Å in the temperature range [100-200] K. [15] This means that the minimal box lengths allowing for the study of the thermal processes are largely within the reach of FPMD, thereby granting legitimacy to the application of a transient method like AEMD.

The structure of g-$GeTe_4$ has been recently studied [16] by Car-Parrinello molecular dynamics (CPMD) [17,18] providing atomic models where the characteristic structure factor and correlation function are in excellent agreement with experimental measurements. The pristine structure of g-$GeTe_4$ adopted in this work contains $N_{at}$=185 atoms in a cubic box with a side $L$=18 Å (see Fig. 1) and it was obtained using the CPMD approach. Within the framework of a study devoted to the impact of different exchange-correlation functionals, [16] with or without account of the dispersion forces, two models of g-$GeTe_4$ were produced by adopting the Perdew, Burke, and Ernzerhof (PBE) [19] and the Becke, Lee, Yang and Parr (BLYP) [20,21] exchange-correlation functionals, respectively. The two schemes were found to have similar performances, the BLYP one being moderately

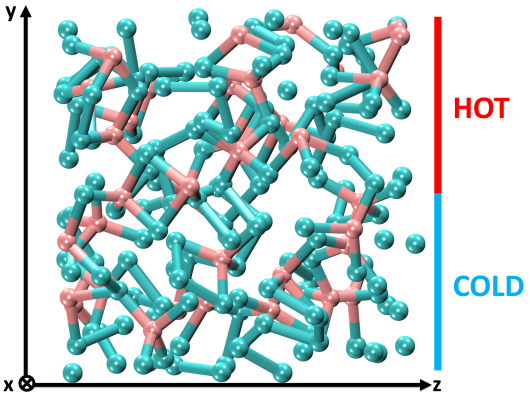


**Fig. 1** Simulation box containing 185 atoms of amorphous $GeTe_4$.

closer to experimental data. The complete set of details for the simulation of g-$GeTe_4$ are available in Ref. [16]. We used the BLYP exchange-correlation functional with a norm-conserving pseudo-potentials [22] describing the valence-core interaction. Long-range dispersion forces are considered by following the formula by Grimme. [16,23] Thermostats are applied to the fictitious electronic degrees of freedom by following the Blochl and Parrinello guidelines. [24]

We have applied the AEMD methodology to g-$GeTe_4$, with a target temperature of $T_t$= 130 K since the MFPs are measured to be the lowest around this temperature. [15] We started by equilibrating the simulation box at $T_t$. Then, we divided the simulation box into two sub-parts along the $y$-direction (Fig. 1). These blocks are intended to be the cold and hot parts allowing for the establishment of the thermal transient. Each block contains around 90 atoms. During a first phase, two distinct Nosé-Hoover [25,26] thermostats are applied to the blocks, with a temperature difference $\Delta T_0$ equal to 50, 100 or 200 K. This step does not require any code development since the multiple thermostats option is already implemented in the CPMD code.

Fig. 2 shows the time evolution of the temperature of the hot and the cold blocks for a temperature difference of 200 K. The temperature gap establishes in a few ps and it is stabilized by the application of the two thermostats along a time slot lasting 35 ps. Then, the thermostats are switched off to allow for the second phase of AEMD to begin. As a consequence, the temperature of the hot (cold) block decreases (increases). Both reach 130 K in 10 ps.

The temperature profile and the temporal evolution of the temperature difference during phase 2 of AEMD are analyzed to check whether they comply with the transient solution of the heat equation. In the conditions of the AEMD

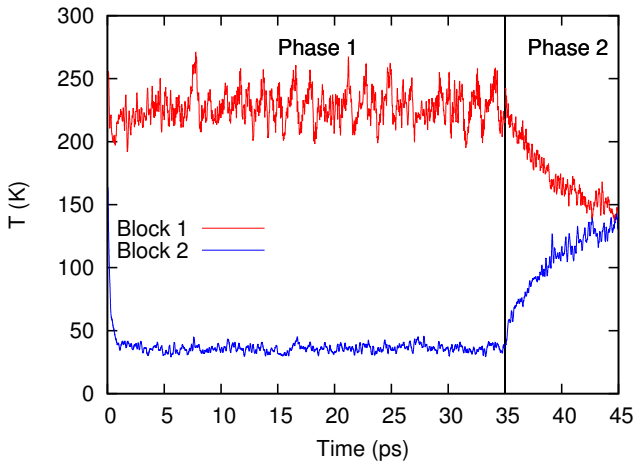


**Fig. 2** Temperature in each block during the two AEMD phases.

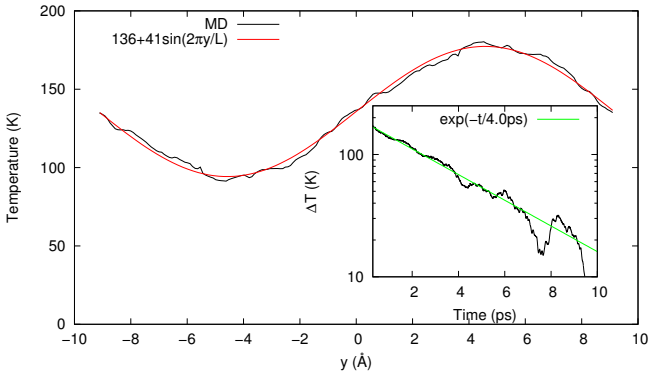


**Fig. 3** Temperature profile and time evolution (from the beginning of phase 2) of the temperature difference (inset) between hot and cold blocks. The dark lines are the CPMD results. The red line is a sine curve adjusted to the CPMD results. The green line in the inset is a decaying exponential adjusted to the CPMD results.

simulations, the solution $T(t,y)$ is a Fourier series[1,27]:

$$T(t,y) = T_l + \sum_{m=0}^{\infty} \frac{2\Delta T_0}{(2m+1)\pi} \sin\left(\frac{2\pi(2m+1)}{L}y\right) e^{-(2m+1)^2 t/\tau}. \quad (1)$$

The dominant contribution of the Fourier series ($m$=0) is a decaying sine :

$$T(t,y) - T_l \propto \Delta T_0 \sin\left(\frac{2\pi y}{L}\right) e^{-t/\tau}. \quad (2)$$

The temperature difference between the two blocks that corresponds to:

$$\Delta T(t) = \frac{2}{L}\int_0^{L/2} T(t,y)dy - \frac{2}{L}\int_{L/2}^{L} T(t,y)dy \quad (3)$$

has a dominant contribution of the form:

$$\Delta T(t) \propto \Delta T_0 e^{-t/\tau}. \quad (4)$$

The temperature difference, shown in the inset of Fig. 3 follows Eq. 4 as exemplified by the linear variation on the semi-log graph. The decay time $\tau$ is extracted by a suitable fit. The temperature profile, averaged along 2 ps (in between 37 and 39 ps of the total simulation time) follows Eq. 2. Since both the temporal evolution of the temperature difference and the temperature profile are consistent with the transient solution of the heat equation, we can exploit the relation between the decay time and thermal conductivity derived from the heat equation:[1]

$$\kappa = \frac{L^2}{4\pi^2}\frac{C_V.\rho}{\tau} \quad (5)$$

where $\rho = N_{at}/L^3$ is the number density. The specific heat $C_V = 3k_B(0.78 \pm 0.02)$ is calculated from the energy fluctuations per atom $\Delta E$ in a $\{NVT\}$ run at 130 K:[28]

$$C_V = \frac{\Delta E^2}{k_B T^2} \quad (6)$$

The thermal conductivity is equal to 0.02 W m$^{-1}$ K$^{-1}$ for the corresponding best fit value of $\tau = 4$ ps (Fig. 3).

It is of interest to ascertain the impact of parameters like the initial temperature difference or the duration of phase 1 on the value of the decay time $\tau$. The results are presented in Fig. 4. For each configuration, $\Delta T(t)$ is fitted to an exponential decay and five different lengths of the time interval are adopted to obtain averages of $\Delta T(t)$. The resulting values of $\tau$ (and the standard deviations) are given in Fig. 4. On the right axis, $\tau$ is converted into a thermal conductivity using Eq. 5.

For instance, in configuration 1, used to obtain the results of Figs. 2 and 3, we applied a single thermostat at $T$ = 130 K to the whole box, before starting the phase 1 with a double thermostat. The difference of the thermostat temperatures is set to $\Delta T_0$: 50, 100 or 200 K. The magnitude of the temperature decay is considerably reduced with $\Delta T_0$=50 K, affecting the precision in the determination of $\tau$. Therefore, we have taken either $\Delta T_0$ =100 or 200 K in the other configurations. In configuration 2, the whole box is first entirely heated at $T_f + \Delta T_0/2$, before a half is cooled at $T_f - \Delta T_0/2$. In this way, the temperature fluctuations are reduced in the hot block at the end of phase 1. To ensure that our results do not depend significantly on the simulation framework, we have also considered the impact of the Nosé thermostat associated with the fictitious electronic degrees of freedom by switching it off during the phase 2 (configuration 3). Finally, in configuration 4,

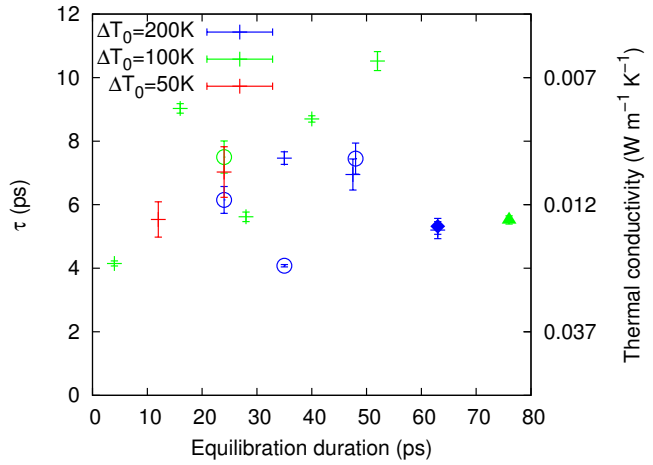


**Fig. 4** Sensitivity of the decay time $\tau$ in phase 2 and thermal conductivity to the parameters of the simulation. In blue, the initial temperature difference is equal to 200 K, in green to 100 K and in red to 50 K. Configuration 1: (+), 2: (o), 3: (♦), 4: (▲).

the frequency of the ionic Nosé thermostats $\omega_i$ is increased from 200 to 350 cm$^{-1}$ in order to optimize the onset of the temperature difference between hot and cold parts.

Fig. 4 shows that the decay time takes values included between 4.0 and 10.5 ps without any clear dependence on the different parameters. The corresponding range for the thermal conductivity is [0.008:0.021] W m$^{-1}$ K$^{-1}$. The thermal conductivity averaged over all configurations standing for the different simulation conditions is equal to 0.013 $\pm$ 0.003 W m$^{-1}$ K$^{-1}$. This averaged value is far from being unrealistic, as it can be understood from the following considerations involving mostly experimental pieces of evidence and (a few) possible details inherent in our simulation approach. Along these lines, it is worth mentioning that Zhang et al.[15] obtained an experimental value of 0.14 W m$^{-1}$ K$^{-1}$ at 130 K using a parallel temperature conductance technique, reportedly leading to an overestimate by 20-25 % of the thermal conductivity compared to a laser flash measurement. This latest experimental framework is closer to our simulation methodology. As an additional issue, the structure and chemical order of such disordered systems are known to be strongly dependent on the conditions of synthesis and processing, resulting in network structures differing by the amount of chemical disorder. A reduced chemical disorder acts to increase the thermal conductivity up to a maximum reached for an ordered crystalline network. For example, in GeTe films, the thermal conductivity goes from 0.23 W m$^{-1}$ K$^{-1}$ for the glass to 3.08 W m$^{-1}$ K$^{-1}$ for the crystal.[29] Zhang et al.[15] claim that the glassy state of $GeTe_4$ is unstable, and the materials has a tendency to crystallize. Again, in the presence of grains, the overall thermal conductivity is likely to be larger than the one pertaining to the glass. On the FPMD simulation side, enhanced chemical disorder is likely to happen since a tendency to overestimate the departures from heterogeneous bonding have been found to characterize chalcogenide glasses,[30–32] in a way that could contribute to obtain lower values for the thermal conductivity. As a final remark on modelling, one cannot neglect the possible impact of size dependent effects due to heat carriers with mean free paths larger than the present box length. Future calculation on large cell sizes will be highly instrumental in this context.

In conclusion, we have exploited the approach-to-equilibrium methodology to calculate the thermal conductivity of a glass with first-principles molecular dynamics in the framework of density functional theory. The setup of the methodology is tractable and straightforward, without requiring any additional implementation in the first-principles CPMD code. We have shown that it is possible to create in a few ps a hot and a cold block by using a double thermostat, and this for an affordable number of atoms ($N_{at}$=185). The approach-to-equilibrium takes a short time, around 10 ps. Both the decay of the temperature difference during this second phase, and the related temperature profile do comply with the heat equation. This allows an access to the thermal conductivity via the decay time. In the specific case of glassy $GeTe_4$, the present approach leads to a calculated thermal conductivity lower than the experimental value. This difference can be rationalized in terms of uncertainties in the experimental structural determination, different amounts of chemical disorder in the corresponding experimental vs. theoretical structures, and specific modelling issues. However, none of them affect the validity and impact of the present approach that proved to be a powerful tool to better understand and quantify thermal phenomena.

## Acknowledgements

Calculations were performed on the facilities of IEMN (clustphy) and on the computational Mesocenter of the University of Strasbourg.

## References

1 E. Lampin, P. L. Palla, P.-A. Francioso and F. Cleri, *J. Appl. Phys.*, 2013, **114**, 033525:1-5.
2 R. Zwanzig, *Ann. Rev. Phys. Chem.*, 1965, **16**, 67-102.
3 P. K. Schelling, S. R. Phillpot and P. Keblinski, *Phys. Rev. B*, 2002, **65**, 144306:1-12.
4 E. Lampin, Q.-H. Nguyen, P.-A. Francioso and F. Cleri, *Appl. Phys. Lett.*, 2012, **100**, 131906:1-4.
5 P. C. Howell, *J. Chem. Phys.*, 2012, **137**, 224111:1-14.
6 Y. He, I. Savić, D. Donadio and G. Galli, *Phys. Chem. Chem. Phys.*, 2012, **14**, 16209-16222.

7 H. Zaoui, P. L. Palla, F. Cleri and E. Lampin, *Phys. Rev. B*, 2016, **94**, 054304:1-9.

8 L. Hu, L. Zhang, M. Hu, J.-S. Wang, B. Li and P. Keblinski, *Phys. Rev. B*, 2010, **81**, 235427:1-5.

9 N. de Koker, *Phys. Rev. Lett.*, 2009, **103**, 125902:1-4.

10 M. Boero, A. Bouzid, S. Le Roux, B. Ozdamar and C. Massobrio, . In *Springer Series in Materials Science 215: Molecular Dynamics Simulations of Disordered Materials. From Network Glasses to Phase-Change Memory Alloys*; C. Massobrio, J. Du, M. Bernasconi and P. S. Salmon, Ed.; Springer International Publishing: Switzerland, 2015; Chapter 2, pp 33-55.

11 A. Marcolongo, P. Umari and S. Baroni, *Nature Physics*, 2016, **12**, 80-84.

12 T. Luo and J. R. Lloyd, *J. Heat Transfer*, 2008, **130**, 122403:1-7.

13 A. S. Henry and G. Chen, *J. Comput. Theo. Nanoscience*, 2008, **5**, 141-152.

14 D. P. Sellan, E. S. Landry, J. E. Turney, A. J. H. McGaughey and C. H. Amon, *Phys. Rev. B*, 2010, **81**, 214305:1-10.

15 S.-N. Zhang, J. He, T.-J. Zhu, X.-B. Zhao and T. M. Tritt, *J. Non-Crystal. Solids*, 2009, **355**, 79-83.

16 A. Bouzid, C. Massobrio, M. Boero, G. Ori, K. Sykina and E. Furet, *Phys. Rev. B*, 2015, **92**, 134208:1-10.

17 R. Car and M. Parrinello, *Phys. Rev. Lett.*, 1985, **55**, 2471-2474.

18 See http://www.cpmd.org, copyright 2000-2017 jointly by IBM Corporation and by Max Planck Institute, Stuttgart.

19 J. P. Perdew, K. Burke and M. Ernzerhof, *Phys. Rev. Lett.*, 1996, **77**, 3865-3868, *Phys. Rev. Lett.*, 1997, **78**, 1396.

20 A. D. Becke, *Phys. Rev. A*, 1988, **38**, 3098-3100.

21 C. Lee, W. Yang and R. G. Parr, *Phys. Rev. B*, 1988, **37**, 785-789.

22 N. Troullier and J. L. Martins, *Phys. Rev. B*, 1991, **43**, 1993-2006.

23 S. Grimme, *J. Comput. Chem.*, 2006, **27**, 1787-1799.

24 P. E. Blöchl and M. Parrinello, *Phys. Rev. B*, 1992, **45**, 9413-9416.

25 S. Nosé, *Mol. Phys.*, 1984, **52**, 255-268.

26 W. G. Hoover, *Phys. Rev. A*, 1985, **31**, 1695-1697.

27 I. R. Vengerov, *J. Eng. Phys.*, 1978, **35**, 866-869.

28 M. E. Tuckerman, *Statistical Mechanics: Theory and Molecular Simulation*; Oxford University Press: Oxford, 2010.

29 R. Fallica, E. Varesi, L. Fumagalli, S. Spadoni, M. Longo and C. Wiemer, *Phys. Status Solidi*, 2013, **7**, 1107-1111.

30 S. Le Roux, A. Bouzid, K. Y. Kim, S. Han, A. Zeidler, P. S. Salmon and C. Massobrio, *J. Chem. Phys.*, 2016, **145**, 084502:1-9.

31 A. Bouzid, S. Le Roux, G. Ori, M. Boero and C. Massobrio, *J. Chem. Phys.*, 2015, **143**, 034504:1-11.

32 C. Massobrio and A. Pasquarello, *Phys. Rev. B*, 2008, **77**, 144207:1-10.